Resonators with manipulated diffraction due to two- and three-dimensional intracavity photonic crystals

M. Peckus,[1] R. Rogalskis,[1] M. Andrulevicius,[2] T. Tamulevicius,[2] A. Guobiene,[2] V. Jarutis,[1]
V. Sirutkaitis,[1] and K. Staliunas[3,4]

[1]*Laser Research Center, Vilnius University, Sauletekio al 10, LT-10222 Vilnius, Lithuania*
[2]*Institute of Physical Electronics, Kaunas University of Technology, Savanorių 271, LT-50131 Kaunas, Lithuania*
[3]*Departament de Fisica i Enginyeria Nuclear, Universitat Politècnica de Catalunya, Colom 11, 08222 Terrassa, Barcelona, Spain*
[4]*Institució Catalana de Reserca i Estudis Avançats (ICREA), Pg. Lluis Companys, 23, 08010 Barcelona, Spain*

We theoretically and experimentally investigate the light dynamics in plane-mirror Fabry-Pérot resonators filled by two-dimensional (2D) and three-dimensional (3D) photonic crystals. It has been predicted that diffraction of such resonators can be manipulated [K. Staliunas, M. Peckus, V. Sirutkaitis, Phys. Rev. A **76**, 051803(R) (2007)]; we study the phenomenon here in detail. In particular, we show the hyperbolic shape angular transmission profiles in case of 2D photonic structure (obtained by one-dimensional modulation of the surface of the mirrors), and quadratic shape transmission profiles in case of 3D photonic structure (obtained by 2D modulation of the mirrors). We develop the theoretical-numerical description of the system using the scattering matrix method and compare numerical results following from the model with the experimental ones.

I. INTRODUCTION

Transverse and the longitudinal modes structure of the homogeneously filled plane-mirror resonators (Fabry-Pérot resonators) are well known. Figures 1(a) and 1(c) illustrate the resonator mode structure for the monochromatic radiation of frequency ω (and correspondingly of the modulus of the wave vector $|\mathbf{k}| = \omega/c = 2\pi/\lambda$). As the presence of the mirrors imposes the resonance conditions on the longitudinal component of the wave vector: $k_\parallel = 2\pi m/(2l)$ (m is the longitudinal-mode number and l is the linear cavity length), then the resonant transverse wave-vector components become $k_\perp = \sqrt{|\mathbf{k}|^2 - k_\parallel^2} = \sqrt{(\omega/c)^2 - (\pi m/l)^2}$, resulting in a system of concentric Fresnel rings in the resonator angular (far-field) transmission profile, counted by the integer values of m. In homogeneous material the character of diffraction is fixed, therefore there is not much freedom in varying the character of angular transmission profile. The mode structure (the system of Fresnel rings) is simply rescaled by varying the optical length of the resonator, i.e., the diffractivity of the resonator.

The idea behind the present article (as well as behind its preceding letter [1]) is that the (transverse and longitudinal) mode structure of the plane-mirror resonator could be substantially modified, filling the resonator by material with periodic in space refraction index, i.e., by a photonic crystal (PC). It is known that the character of diffraction can be substantially modified in the bulk propagation through the material with periodic in space modulation of the refraction index of the media: the dominating orders of diffraction can change the sign or convert to zero, resulting in the latter case to the effect of the self-collimation or subdiffraction [2–6]. This allows expecting that the mode structure of the resonator will be also respectively modified by the intracavity refraction index modulation. As the angular transmission profile of the resonator is closely related with its transverse-mode structure, then the shape of the resonator angular transmission profile should also strongly depend on the char-

acter of the intracavity refraction index modulation. In particular the angular transmission profile can be broadened or narrowed with respect to that of "homogeneous" resonator, resulting in subdiffractive and superdiffractive resonators [1]. In the present article we perform a systematic numerical and experimental study of the angular transmission properties in such resonators with intracavity refraction index modulation,
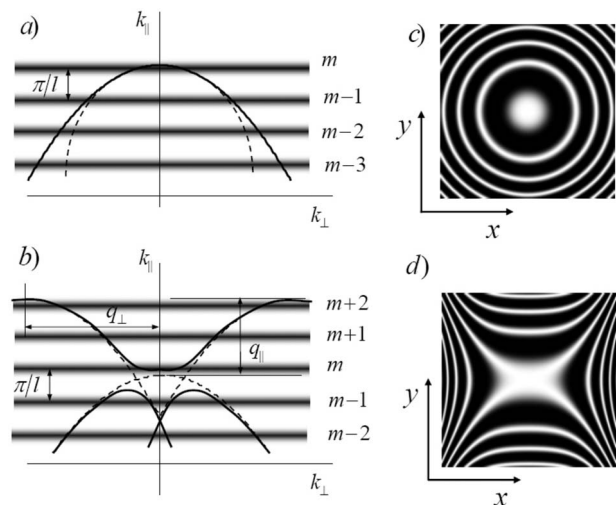

FIG. 1. The spatial dispersion curves of the monochromatic plane waves in (a) homogeneous media and (b) of the Bloch modes in photonic crystals. The dispersion curve (b) is taken from [1], i.e., calculated by a standard technique of harmonic wave expansion. The dashed lines in (b) indicate the dispersion curves of the uncoupled plane waves [or equivalently of the Bloch modes in the limit of vanishing index modulation ($s \to 0$)]. The thick fuzzy lines in (a) and (b) indicate the resonances of the resonator as characterized by the condition of the longitudinal component of the wave vector $k_\parallel = 2\pi m/(2l)$. (c) the Fresnel ring structure of the homogeneously filled resonator and (d) shows the mode structure for the resonator with index modulation in one transverse direction.
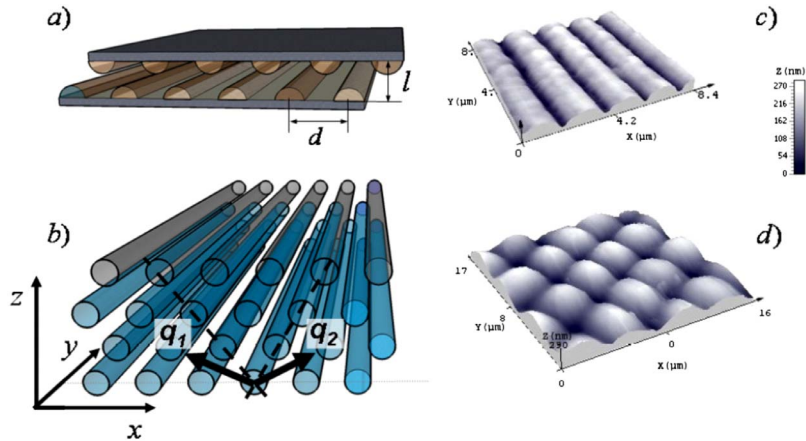
FIG. 2. (Color online) The principal scheme of the resonator used in (a) experiments and (b) the corresponding unfolded PC structure in case of 1D modulation of the mirrors (2D intracavity PC). The dashed lines indicate crystallographic axes of the unfolded PC structure and the arrows represent the vectors of the reciprocal lattice. The microscope images of the mirror surfaces in case of (c) 1D modulation and (d) 2D modulation of mirror surfaces (corresponding respectively to 2D and 3D intracavity PCs).

or in other words the resonators filled by two-dimensional (2D) and three-dimensional (3D) PCs.

Figures 1(b) and 1(d) illustrate the idea that the Fresnel ring structure could be substantially modified if the diffraction of resonator is manipulated due to the periodic intracavity refraction index modulation. Here the 2D intracavity PC is considered, i.e., the index is considered to be modulated in one transverse and in one longitudinal direction (with respect to the optical axis of the resonator). In particular the relatively broad angular areas of the resonances can be expected along the optical axis of the resonator when the plateau appears on the spatial dispersion curves [Fig. 1(b)] instead of the relatively narrow rings or a central spot [Fig. 1(a)]. The 2D angular resonance profiles are more involved. Figure 1(d) illustrates the dispersion surface accounting for the two transverse dimensions, where the refraction index is modulated in one transverse direction only (2D PC). As the spatial dispersion surface resembles the saddle, then the resonances, being the horizontal cuts of the dispersion surface, result in the hyperbolalike angular transmission structure—in a strong contrast with the Fresnel ring structure of the homogeneously filled resonators in Fig. 1(c).

The Fig. 1(d) illustrates that even in case of the 2D intracavity PC the angular resonance structure (and angular transmission profile) becomes involved. In general the resonator can contain the 3D PC, which, depending on the symmetry of the crystal, can modify the dispersion surface in a more complicated way. The article presents a study, theoretical and experimental, of such resonators, filled by 2D and 3D photonic crystals.

The previous study of the resonator filled by PCs in [1], considered the 2D intracavity PCs only. Here we extend the study to the 3D PC cases. We also note that the light dynamics in the resonator modulated in a transverse direction only (no longitudinal index modulation) were studied in [7] by applying the mean-field models. Here in our study, both in 2D and 3D PC cases, the longitudinal modulation of the refraction index is considered (the longitudinal modulation index is necessary in order to obtain the subdiffractive, or self-collimating, regimes [2–6]). The presence of the longitudinal modulation of the refraction index does not allow application of the mean-field models, such as, e.g., in [7]. Therefore we developed a theoretical approached based on the multiple-scattering matrix analysis. This analysis allows

taking into account the multi-longitudinal-mode structure (multirings). (We note that in [1] only the central resonance was considered as is usual in simplified single-longitudinal-mode models.) Apart from the qualitative differences from [1] (the 3D intracavity PC in theoretical and experimental study, also the multi-longitudinal-mode theoretical model) we note the quantitative differences, in that much smaller spatial periods of the gratings were used in experiments in the present work (2 μm in transverse direction in 2D case, and 4 μm in 3D case). Therefore the structures used are much closer to the real PC microresonator (We note that previously in [1] the transverse modulation period was 15 μm, and the length of the resonator was 0.5 mm, which was a "magnified model system" of the real PC resonator). Also the finesse of the resonator in [1] was very low, which resulted in the superdiffractive behavior only (the angular width of the resonator was narrower than that of the homogeneous resonator). Here we succeeded in approaching the subdiffractive regime too.

The paper is organized as follows. First in Sec. II we describe the scheme used in experiments. In Sec. III we derive the multiple-scattering matrix model, used to calculate the mode structure and the angular transmission profile of the PC resonator. Finally we present the numerical and experimental results of our study (Sec. IV), for the case of the mirror surface modulation in one transverse direction (Sec. IV A) and in two transverse dimensions (Sec. IV B), followed by the conclusion in Sec. V.

II. RESONATOR WITH THE INTRACAVITY PC

The idea for such a resonator with intracavity PC is illustrated in Fig. 2. Instead of creating a modulation of the refraction index in both the longitudinal and transverse directions of the intracavity media, we modulated instead the surfaces of the mirrors in [Fig. 2(a)]. The mirrors, as shown in Fig. 2(a) are shifted one with respect to another by a half of period. This, in an unfolded structure of such a resonator [Fig. 2(b)], results in a 2D PC: the wave resonating along the optical axis of the resonator is experiencing the periodic index of refraction both in longitudinal and transverse directions. The lateral shift of the mirrors results in a propagation along the diagonals of the rhombs of unfolded lattice of refraction index in the case of modulation in one transverse

direction. We note that such a geometry (the propagation along the diagonals of a square lattice) is suitable for the self-collimation [2], and for the respective manipulation of the diffraction [3–6]. This is the reason why we have chosen such a geometry (in particular the laterally shifted mirrors).

The mirrors of the resonator used in experiments are shown in the Figs. 2(c) and 2(d), for the cases of modulation in one and two transverse dimensions, respectively. For the fabrication of the mirrors the low roughness ($\lambda/20$) substrates were used. Working side of a mirror was covered by high reflection (98.5%) coatings and the other side with antireflection. The modulation of the surface of the mirror was achieved by photolithography technology. The surfaces of the mirrors were first covered with a thin film of ma-P S1205 positive photoresist (of ≈ 0.3 μm thickness, of $n=1.58$ index of refraction) using spin coating technique (4500 rpm). Next, in 1D modulation case, using conventional contact optical photolithography the resist was exposed and developed forming the 1D periodical structure of the period $d=2$ μm in 1D modulation case. In the 2D modulation case a film of a resist was exposed twice with 90° rotated template. In this way $d_x=d_y=4$ μm modulation was produced. The width of the etched groves was approximately the half of their period $\approx d/2$ so the coatings on the mirror act as the phase grating. Subsequently the mirrors were baked ($T=1000$ C) in order to smoothen the profile of the photoresist, and to make the surface modulation as close as possible to the harmonic one [see Figs. 2(c) and 2(d)].

Precise optomechanics or/and 3D Piezo translator were used for cavity alightment and attenuation. The distance between the mirrors (the linear length of the resonator) was varied in the range $l=5-40$ μm in accordance to the calculations (presented below). The mirrors were shifted one with respect to another by the half of the grating period in order to mimic the 2D photonic crystal with the optical axis directed along the diagonals of rhombs [see Fig. 2(b)] in case of 1D modulation. In 2D modulation case the care was taken to shift the periodic structure in both transverse directions. In the unfolded structure the propagation of light succeeded along the diagonals of the cubic structure. The self-collimation in 3D is most prominent along the diagonals of the cubic structure (as calculated in linear cases [8], as shown experimentally [9], and as predicted in nonlinear case [10]). The resonator was illuminated by the cw laser beam (wavelength 532 nm, beam width 2.5 mm, power 15 mW). A diffuser was placed in front of the front mirror of the resonator in order to generate broad spatial spectrum of the illuminating radiation. Transmitted radiation was recorded by using lens and charge-coupled device (CCD) or screen and photo camera. A lens of 58 mm focal distance was used to collect the transmitted radiation into CCD camera for the far-field recording.

III. THEORETICAL MODEL

For the theoretical-numerical analysis of the resonator modes we developed an approach based on the multiple-scattering matrix technique. We analyze a round trip propagation of light along the resonator and calculate the transfor-

mation of the field on each of the elements consecutively: (i) the diffraction on the modulated surface of the mirror; (ii) the free space propagation between the mirrors (diffraction in homogeneous material); (iii) the lateral shift of the periodic structure of the mirrors one with respect to another; (iv) the partial reflections from the mirrors. After calculating the field transformation in a resonator roundtrip (by applying the transformation operators, i.e., by multiplying by corresponding transformation matrices), we calculate the resonator transmission matrix by the standard techniques: by adding the entering plane wave to the resonators and by searching for a stationary state. This is essentially a classical approach to calculate the mode structure of the homogeneously filled Fabry-Pérot resonator, with the difference that the field transformations on each of the element in the resonator now are not the scalars but operators (represented by matrices).

The periodic modulation of the mirror surface results in a set of diffraction components in reflected light with transverse the components of the wave vectors $\vec{k}_\perp + \vec{q}_{m,n}$, here $\vec{k}_\perp = (k_x, k_y)$ is the transverse wave vector of the incident light and $\vec{q}_{m,n} = (mq_x, nq_y)$ are the multiples of the modulation wave vector. Strictly speaking one should consider all the possible field harmonics, however it comes out that the consideration of the central component plus the first-order sidebands is sufficient [1]. For 1D modulation of the mirrors this results in three components (as considered in [1]) for 2D square modulation of the mirrors) in five components [10]. We approximate, therefore, the optical field in the following way:

$$A(\mathbf{r}) = e^{i(k_x x + k_y y)}(a_{0,0} + a_{-1,0}e^{-iq_x x} + a_{+1,0}e^{iq_x x} + a_{0,-1}e^{-iq_y y}$$
$$+ a_{0,+1}e^{iq_y y}). \tag{1}$$

The field, for convenience, is further represented by the column-vector of plane-wave components,

$$\vec{A} = (a_{0,-1}, a_{-1,0}, a_{0,0}, a_{+1,0}, a_{0,+1})^T. \tag{2}$$

The $q_\perp = (q_x, q_y)$ are the wave vectors of the index modulation in the transverse direction (the field is expanded in its harmonics). In general q_x and q_y can be different one from another, but throughout the article we will consider the square lattice $q_x = q_y = q_\perp$ in the 2D modulation case. Plane-wave set (2) is tilted with respect to the optical axis, as represented by the factor in Eq. (1) with nonzero $\vec{k}_\perp = (k_x, k_y)$.

Next we list consecutively the field transformations in the resonator roundtrip.

Scattering by the phase grating. The periodically modulated phase of the field on the reflection of the surface of the mirror couples the components of the field vectors. For the harmonic modulation the coupling occurs between the central component $a_{0,0}$ and the sidebands in this five harmonic model. We introduce the phenomenological scattering coefficients s_x and s_y into both transverse directions, respectively. In the square grating (2D) case $s_x = s_y = s$, and the 1D modulation case by $s_x = s$, $s_y = 0$. The scattering s can be linked to microscopic parameters of the coating, as the depth of the modulation, and the refraction index of the photoresist. However it is more convenient to keep the macroscopic scattering

parameter, as it is directly linked with the experimentally accessible diffraction efficiency of the grating (s is the square root of the scattering intensity into the sidebands). The scattering matrix is

$$\hat{S} = \exp \begin{pmatrix} 0 & 0 & is_y & 0 & 0 \\ 0 & 0 & is_x & 0 & 0 \\ is_y & is_x & 0 & is_x & is_y \\ 0 & 0 & is_x & 0 & 0 \\ 0 & 0 & is_y & 0 & 0 \end{pmatrix}. \qquad (3)$$

More convenient (for numerical purposes) is however to simplify the scattering operator, which in Eq. (3) is the matrix exponent. The simplification is being done by series expansion of Eq. (3), which truncated to three expansion terms reads

$$\hat{S} = \begin{pmatrix} 1 - s_y^2/2 & -s_x s_y/2 & is_y & -s_x s_y/2 & -s_y^2/2 \\ -s_x s_y/2 & 1 - s_x^2/2 & is_x & -s_x^2/2 & -s_x s_y/2 \\ is_y & is_x & 1 - s_x^2 - s_y^2 & is_x & is_y \\ -s_x s_y/2 & -s_x^2/2 & is_x & 1 - s_x^2/2 & -s_x s_y/2 \\ -s_y^2/2 & -s_x s_y/2 & is_y & -s_x s_y/2 & 1 - s_y^2/2 \end{pmatrix}. \qquad (4)$$

Simplified scattering matrix (4) is an approximate expression, and therefore does not preserve the energy precisely during the scattering process. The absolute values of eigenvalues of matrix (4) are not equal to unity as the truncation introduces errors in the absolute values of eigenvalues of the order of $O(s^4)$. For the experimental values used $s \approx 0.2 \div 0.3$ the nonconservation of the energy is therefore negligible.

Free propagation. The free propagation over the linear length of the resonator is considered by the paraxial propagation equation

$$\partial_z A(\mathbf{r}) = \frac{i}{2k_0} \nabla_\perp^2 A(\mathbf{r}), \qquad (5)$$

where $\nabla_\perp^2 = \partial^2/\partial x^2 + \partial^2/\partial y^2$ is the Laplace operator acting in the transverse plane. Substitution of expansion (1) into (5) yields the equation system

$$\partial_z a_{m,n} = -\frac{i}{2k_0}[(mq_x + k_x)^2 + (nq_y + k_y)^2]a_{m,n}. \qquad (6)$$

The integration of Eq. (6) over one linear resonator length results to the diagonal transformation matrix

$$\vec{P} = e^{ilk_0}\text{Diag}(e^{-iL(k_y + q_y)^2 - iLk_x^2}, e^{-iL(k_x + q_x)^2 - iLk_y^2}, e^{-iLk_x^2 - iLk_y^2},$$

$$e^{-iL(k_x - q_x)^2 - iLk_y^2}, e^{-iL(k_y - q_y)^2 - iLk_x^2}). \qquad (7)$$

Here $L = l/(2k_0)$ is the normalized length of the resonator, representing its diffraction.

Lateral shift of the mirror. We account for the lateral shift of the grating [determined by $\vec{m} = (m_x, m_y)$] using the following trick. We fix the reference frame with the position of the first mirror. Then, for the calculation of the scattering from

the laterally shifted second mirror we change the reference frame, by applying the operator

$$\vec{M} = \text{Diag}(e^{+im_y q_y}, e^{+im_x q_x}, 1, e^{-im_x q_x}, e^{-im_y q_y}). \qquad (8)$$

Then, after calculation the scattering on the second mirror [by using Eq. (3) or (4)] in the new reference frame), we restore the original reference frame, by applying $\vec{M}^{-1}$.

Resonator mirrors. Since the reflectivity is the same for all harmonic components of the wave, it is accounted in a standard way—by multiplication by a scalar r. Without losing generality in theory, and in accordance to our experiment, we consider the both mirrors of the same reflectivity.

Resonator roundtrip. The variation in the field in a resonator roundtrip is calculated by applying consecutively all the operators discussed above,

$$\hat{R} = r^2 \hat{P}\hat{M}^{-1}\hat{S}\hat{M}\hat{P}\hat{S}. \qquad (9)$$

Resonator transfer function. The plane wave entering into the resonator is denoted in this vector form by $\vec{A}_0 = (0, 0, B_0, 0, 0)^T$. Then we calculate the radiation balance in one resonator roundtrip, and analogously to the homogeneous Fabry-Pérot case, we obtain

$$\vec{A} = t(\hat{1} - \hat{R})^{-1}\vec{A}_0 \qquad (10)$$

for the radiation at the entrance mirror. The only difference from the homogeneous Fabry-Pérot case is that here we deal with the vectors of the wave components and transformation matrices, instead of complex scalar factors. Finally the resonator transmission matrix is

$$\hat{T} = t^2(\hat{1} - \hat{R})^{-1} = t^2(\hat{1} - r^2\hat{M}^{-1}\hat{P}\hat{S}\hat{M}\hat{P}\hat{S})^{-1}. \qquad (11)$$

The transmission for the homogeneous component is given by the element $T_{0,0}$ of transfer matrix (11). The scattering of the resonator into the sidebands harmonics is described by the corresponding off-diagonal column elements of the matrix: by $T_{-1,0}$ and $T_{+1,0}$ into the diffraction components in x direction, and by $T_{0,-1}$ and $T_{0,+1}$ into the diffraction components in y direction.

IV. RESULTS

The resonator configuration was build aiming to the subdiffractive condition, i.e., the flattening of the dispersion curve as illustrated in Fig. 1, which occurs at around the resonance conditions for all the significant harmonic components. Although the final expression for resonator transmission function (11) does not allow analytical interpretation of the results, the inspection of free-propagation matrix (7) allows evaluating the parameters for this multiple resonance. The simultaneous resonance of all harmonic components is possible if the different harmonic components belong to the different longitudinal modes: the central mode $a_{0,0}$ belongs to a particular longitudinal mode n, and the sideband modes belong to the longitudinal mode with the index $n-1$. From Eq. (7) it follows that the conditions must hold: $lk_0 \approx \pi n$ (the resonance for the central component), and $Lq_x^2 = Lq_y^2 \approx \pi$ (the resonance for the sidebands). The latter means $lq_{x,y}^2/k_0$
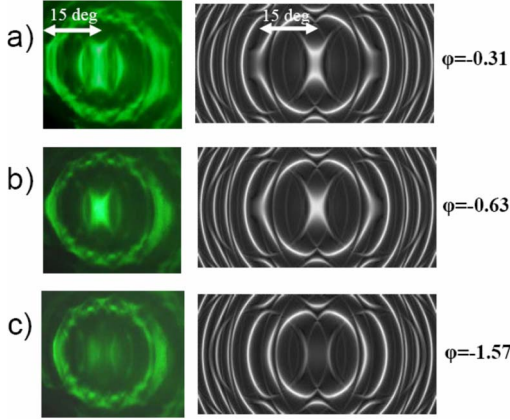
FIG. 3. (Color online) Far field of the radiation transmitted through the resonator with 1D modulated mirror surface as recorded experimentally and calculated numerically from Eq. (11). The lateral shift of the mirrors is a half of modulation period. Parameters used in numerics: $S=0.4$; $T=0.2$; $d=4.0$; $m=\pi$; the resonator roundtrip phase was varied to fit the experimental plots.

$\approx 2\pi$, or equivalently $l\lambda/d_{x,y}^2 \approx 1$, where $d_{x,y}=2\pi/q_{x,y}$ are the corresponding spatial periods of the modulation of the surfaces of the mirrors, and l (we repeat) is the linear length of the resonator.

The latter conditions were indicators for selecting the resonator length in our experiments. The "rough tuning" of the resonator length around the critical one $l_{cr}=d_{x,y}^2/\lambda$ ensures the multiple resonance condition, i.e., all field harmonics are simultaneously in or out of the resonance, depending on the fine tuning of the resonator. The other condition $lk_0 \approx \pi n$ was considered for the fine (submicron) tuning of the resonator length in order to simultaneously tune all harmon-
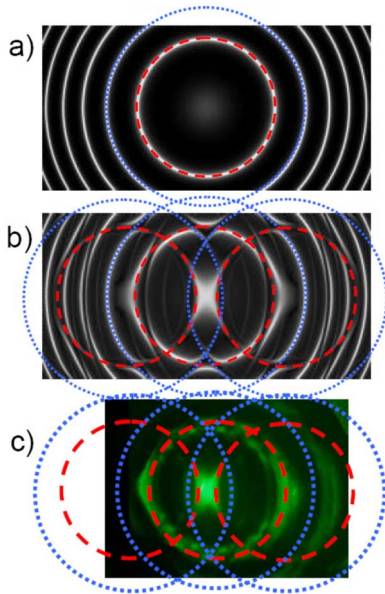

FIG. 4. (Color online) Ring structure of the resonator with 1D modulated mirrors. (a) Cavity ring structure with the absence of a modulation ($S=0$); (b) Numerical simulation of PC resonator ($S=0.4$). Parameters: $T=0.2$; $d=4.0$; $m=\pi$; $\varphi=-0.63$; (c) Experimentally obtained resonator transmission. Rings are the same as (a)–(b) (asymmetry is experimental artifact.)
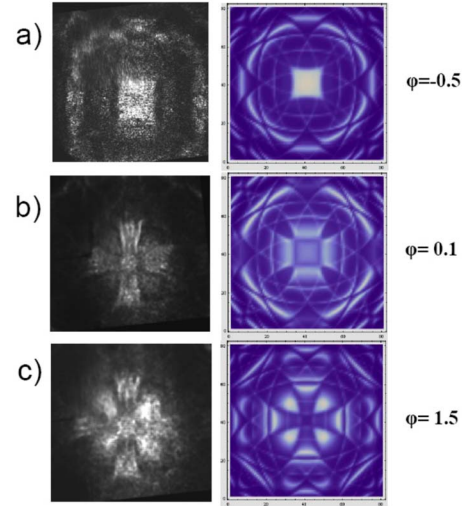

FIG. 5. (Color online) Far field of the radiation transmitted through the resonator with 2D modulated mirrors as recorded experimentally, and calculated numerically [Eq. (9)]. The lateral shift of the mirrors is a half of modulation period in both directions ($mx=my=\pi$). Parameters: $S=0.4$; $T=0.2$; $d=4.5$.

ics to the resonance. The fine tuning is characterized by the roundtrip phase of the resonator: $\varphi=2lk_0-2\pi n$.

A. 1D modulation of the mirror surfaces

In 1D experiments the period of the modulation of mirror surface was ($dx=2 \ \mu$m), which implies the critical cavity length of $l_{cr}=d^2/\lambda=7.5 \ \mu$m. Figure 3 shows the resonator transmission function obtained at around the critical length of the resonator, and by varying the fine tuning condition, as characterized by the roundtrip phase $\varphi=2lk_0-2\pi n$. The roundtrip phase in experiments could not be directly determined, and was indirectly restored from the comparison with the corresponding numerical plots (with explicitly defined phase).

The far field of the transmitted radiation as recorded experimentally (left column in Fig. 3) is in good qualitative correspondence with calculated numerically (right column in Fig. 3). Case (b) corresponds to the multiple resonance of all three waves, i.e., to the case when the frequency of the plateau of dispersion curve is fine tuned to the resonance. Cases (a) and (c) are characteristic for situations when the resonator is fine tuned to the opposite directions from the resonance.

The multiple resonance conditions can be interpreted also in a geometric way. The rough tuning discussed above condition means that the radius of the first Fresnel ring (at resonance) is approximately equal to diffraction angle of a grating of the mirror. The fine tuning condition means that the Fresnel rings from two diffracted components overlap on the spot of the central component. Figure 4 shows the ring structure of the PC cavity, illustrating the above discussed resonance condition. The ring structure around the diffraction maxima is clearly visible in both numerical and experimental field distributions, and the resulting far-field transmission pattern can be well interpreted with the help of the system of the Fresnel rings.
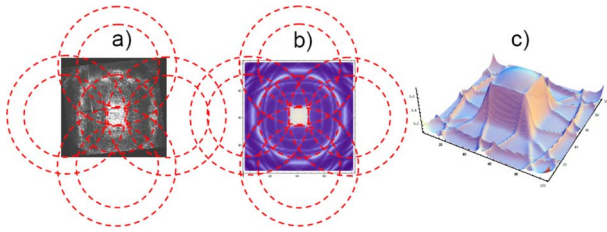
FIG. 6. (Color online) Ring structure of 2D modulated mirrors cavity. (a) Experimental results and (b) numerical simulation as taken from Fig. 5. Dashed rings indicate imaginary place of transmission rings around diffraction maxima. (c) shows 3D resonator transmission structure, showing the role of two resonance rings, as obtained from numerics of (11).

B. 2D modulation of the mirror surfaces

In 2D experiments the periods of the modulation of mirror surface was (dx=4 μm, dy=4 μm), (quadratic structure), which implies the critical cavity length of $l_{cr}=d^2/\lambda$ =30 μm. Figure 5 shows the resonator transmission function obtained at around the critical length of the resonator, and by varying the fine tuning condition.

Also in 2D modulation case a good qualitative correspondence with numerically obtained results was observed. Here again, the resonant case was obtained, characterized by relatively flat (homogeneous) and broad resonator transmission function. This case is analogous to the case in Fig. 3(b), however here obtained as a simultaneous resonance of the five waves. Also in analogy to 1D cases, the typical off-resonance transmission distribution were obtained, and shown in Figs. 5(b) and 5(c).

The multiple resonance condition, and the appearance of plateau can be also interpreted in a geometric way, such as in 1D modulation case. Differently from the 1D case, here it seems that the most homogeneous plateau appears under participation of the two resonant rings from the diffraction maxima, as indicated in Fig. 6. This means that the longitudinal $n-2$ modes also participate in formation of subdiffractive pattern.

The resonator transmission pattern was sensible with respect to the lateral shift of the resonator mirrors one with respect to another. Figure 7 reports the result of study of the lateral shift. As expected, the lateral shift by the value differ-
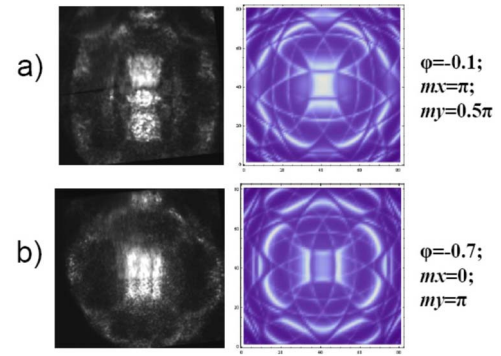

FIG. 7. (Color online) Far field of the radiation transmitted through the resonator with 2D modulated mirrors and different lateral shift as recorded experimentally and calculated numerically [Eq. (11)]. Parameters: S=0.4; T=0.2; d=4.5;

ent than $m_{x,y}=\pi$, 0.5π results in asymmetric pattern with respect to the direction with broken symmetry [Fig. 7(a)]. The lateral shifts of $m_{x,y}=0$ and $m_y=\pi$ result in different patterns, as shown in Fig. 7(b).

V. CONCLUSIONS

Concluding, we build the PC resonator with the intracavity modulation of refraction index, i.e., the resonator containing one longitudinal period of the PC. We develop the method of the calculation of such resonator, based on the scattering matrix theory, and we reproduce the experimentally observed transmission patterns by numerical integration of the developed model. We demonstrate experimentally the basic properties expected, i.e., the hyperbolic shape transmission patterns in case of 1D modulation of the mirror surfaces, and square shape patterns in case of 2D modulation of the mirror surfaces.

The PC resonator shows basic properties expected—the relatively flat angular transmission profile. The maximum transmission area is of quadratic shape, due to a quadratic symmetry of the modulation of the mirror surfaces. The more symmetric modulation patterns (hexagonal or octagonal) are expected to result in a more isotropic transmission spot.

[1] K. Staliunas, M. Peckus, V. Sirutkaitis, Phys. Rev. A **76**, 051803(R) (2007).

[2] H. Kosaka, T. Kawashima, A. Tomita, M. Notomi, T. Tamamura, T. Sato, and S. Kawakami, Appl. Phys. Lett. **74**, 1212 (1999).

[3] T. Pertsch, T. Zentgraf, U. Peschel, A. Brauer, and F. Lederer, Phys. Rev. Lett. **88**, 093901 (2002).

[4] D. N. Chigrin, S. Enoch, C. S. Torres, and G. Tayeb, Opt. Express **11**, 1203 (2003).

[5] R. Iliew, C. Etrich, U. Peschel, F. Lederer, M. Augustin, H. J. Fuchs, D. Schelle, E. B. Kley, S. Nolte, and A. Tünnermann, Appl. Phys. Lett. **85**, 5854 (2004).

[6] K. Staliunas and R. Herrero, Phys. Rev. E **73**, 016601 (2006).

[7] D. Gomila, R. Zambrini, and G. L. Oppo, Phys. Rev. Lett. **92**, 253904 (2004); D. Gomila and G. L. Oppo, Phys. Rev. E **72**, 016614 (2005).

[8] R. Iliew, C. Etrich, and F. Lederer, Opt. Express **13**, 7076 (2005).

[9] Z. Lu, S. Shi, J. A. Murakowski, G. J. Schneider, C. A. Schuetz, and D. W. Prather, Phys. Rev. Lett. **96**, 173902 (2006).

[10] K. Staliunas, R. Herrero and G. J. de Valcárcel, Phys. Rev. A **75**, 011604(R) (2007).